Polymer Bulletin 60, 791–798 (2008)
DOI 10.1007/s00289-008-0908-8

Polymer Bulletin

# Crystal morphology of rapidly cooled isotactic polypropylene: A comparative study by TEM and AFM

**Qamer Zia[1], René Androsch[1] (✉), Hans-Joachim Radusch[1], Elisabeth Ingolič[2]**

[1]Martin-Luther-University Halle-Wittenberg, Center of Engineering Sciences, 06099 Halle/S., Germany
[2]Graz University of Technology, Research Institute for Electron Microscopy, 8010 Graz, Austria

E-mail: rene.androsch@iw.uni-halle.de; Fax: +49 3461 46 3891

Received: 4 January 2008 / Revised version: 30 January 2008 / Accepted: 4 February 2008
Published online: 20 February 2008 – 

## Summary

The morphology of crystals, formed at the surface and in the bulk of rapidly cooled and subsequently at elevated temperature annealed films of isotactic polypropylene (iPP) was analyzed by transmission electron microscopy (TEM) and by atomic force microscopy (AFM). Both techniques show a lamellar crystals after melt-crystallization at 12 K $s^{-1}$, and a nodules after melt-crystallization at 750 K $s^{-1}$. The morphology of crystals is independent on the position of the investigated film of thickness of 100 μm, suggesting (a) that the crystallization at the surface is not affected by the use of a glass substrate for preparation, and (b) that the temperature-gradient during primary crystallization is sufficiently small to ensure identical structure at the surface and in the bulk. AFM suggests a larger size of crystals than TEM, in particular if the absolute size of objects approaches the dimensions of the used tip of the AFM. If the absolute size of objects is distinctly larger, then AFM and TEM yield nearly identical dimensional information.

## Introduction

The structure of isotactic polypropylene (iPP) depends on the rate of cooling on melt-crystallization [1,2]. Melt-crystallization at a rate lower than about $10^1$ K $s^{-1}$, in absence of special nucleation agents, results in formation of monoclinic α-crystals of lamellar geometry. Melt-crystallization at a rate faster than about $10^2$ K $s^{-1}$, in contrast, yields globule-shaped mesomorphic domains. Lamellar crystals and mesomorphic nodular domains can simultaneously be observed after cooling at a rate between $10^1$ and $10^2$ K $s^{-1}$. Recently, the morphology, i.e., the shape and size of mesomorphic domains was quantitatively and systematically analyzed as a function of the rate of cooling on primary melt-crystallization, and as a function of the condition of subsequent annealing [3,4]. The size of the nodular mesomorphic domains is almost independent on the cooling rate, being only slightly decreased from about 20 nm, after melt-crystallization at $10^2$ K $s^{-1}$, to 15-18 nm, after melt-crystallization at $10^3$ K $s^{-1}$. Subsequent annealing at elevated temperature results in a major increase of the size of

crystals to almost 50-60 nm, in particular if the annealing is performed at temperatures close to final melting, i.e., at temperatures above about 400 K. The shape of the initially nodular domains, however, is unchanged after annealing, i.e., the nodules seem to grow in all directions such that the aspect ratio is preserved.

Initially, we explored the morphology of ordered domains/crystals by atomic force microscopy (AFM). Since AFM mainly provides information about the structure and properties at or near the surface [5], we attempt in the present study to confirm or discard identity of surface and bulk structures by application of transmission electron microscopy (TEM). The need to employ TEM for a complete analysis of the structure is twofold. First of all, surface and bulk structures can vary due to different conditions of crystallization. Crystallization, since temperature-dependent [6], is affected by gradients of temperature or rate of cooling during preparation of films, respectively, or by the presence of substrates at the surface [7,8]. Secondly, quantitative analysis of morphological parameters of crystals may depend on instrumentation. There are several studies on polymeric and non-polymeric systems which yielded different results when analyzed by AFM and by TEM [9-14]. In general, objects seem to appear larger in AFM-analysis than in TEM-analysis. Major reasons may be the geometry of the tip in AFM, which is used for mechanical interaction with the specimen, and the phenomenon of over-etching during preparation in TEM-analysis [15,16]. Examples for observation of an apparent mismatch between AFM and TEM data in polymeric systems include the thickness of lamellae in melt-extruded films of high-density polyethylene [9], the size of nanospheres of polystyrene [10], the long period in stacks of lamella and the size of rubber-particles in polymer blends [11,12].

Summarizing the scope of this study, we intend to prove identical morphology of mesomorphic domains/monoclinic crystals at the surface and in the bulk of initially rapidly cooled, and subsequently annealed iPP. Indifferent crystal morphology at the surface and in the bulk rules out an effect of mica or glass substrates on surface-crystallization. These substrates we used in the past for generation of sufficiently smooth surfaces for optimum AFM-analyses, assuming absent epitaxial growth of iPP-crystals. The effect of a temperature gradient during preparation of films is estimated by monitoring the evolution of structure as a function of the position in direction of the film thickness. Finally, we attempt to evaluate the effect of instrumentation by comparison of structure, observed at nearly identical position within the sample by AFM and TEM.

## Experimental

### *Materials*

In the present study is used an iPP with a mass-average molar mass of 373 kg $mol^{-1}$ and a polydispersity of 6.2, provided by Montell Polyolefins. Films of thickness of 100 μm were prepared with a special device for controlled rapid cooling. In this particular study, we used specimens which were melt-crystallized at cooling rates of 12 and 750 K $s^{-1}$, yielding thin lamellar crystals, and nodular crystals, respectively. The annealing experiments were done on a Leitz hot-stage 1350, in combination with a Rheometric Scientific temperature controller. Each annealing experiment was done with a new sample. Further details of the characteristics of the material and of the sample preparation are described elsewhere [3,4].

*Instrumentation*

*TEM.* The bulk morphology of the films was analyzed using a TEM Tecnai G2 (FEI), operated at 120 kV. Images were collected with a Bioscan CCD Camera, Model 792 (Gatan). The 100 μm films were embedded in Epofix (Struers), and subsequently contrasted with Rutheniumtetroxide for a period of about 12 hours [17]. Thin sections of 75-85 nm thickness of the cross-section of the films were prepared at ambient temperature. using an Ultracut microtome (Leica), equipped with a 45°-diamond knife (Diatome). Images were collected from the center and near the edges of the thin sections. Zoomed-in TEM images are shown as insets and are digitally filtered to enhance the contrast without distorting the features present in the original images.
*AFM.* The surface-structure of the films was analyzed using a Quesant Q-Scope 250 AFM, equipped with a 40 μm × 40 μm scanner. Standard silicon cantilevers NSC 16 with a resonant frequency and force constant of about 170 kHz and 40 N $m^{-1}$, respectively, were used for scanning. Phase- and height-mode images were collected simultaneously in tapping mode at ambient temperature, with the figures showing the phase images. The film surface was not etched additionally by chemicals.

## Results

Figure 1 shows the structure of iPP after non-isothermal melt-crystallization at a rate of cooling of 12 K $s^{-1}$. The left image was taken by AFM, and the center and right images were collected by TEM. All micrographs represent an area of 500 nm × 500 nm. The insets are enlargements and show an area of 100 nm × 100 nm. The AFM-image shows the structure at the surface of the film of 100 μm thickness, which, during crystallization, was in contact with glass. Melt-crystallization at 12 K $s^{-1}$ on the glass substrate results in formation of lamellae, which are recognized as the bright, stick-like objects in the AFM-micrograph. Additionally, a few particle-like objects can be identified. The center and right TEM-images in Figure 1 show the structure in the center and near the surface of the film, respectively. Both TEM-images show lamellae, similar as were observed by AFM. The dimensions of lamellae, however, are considerably smaller when analyzed by TEM. Manual estimation of the thickness of lamellae yields values of 7-8 and 4-5 nm for the AFM and TEM analyses, respectively. These data are confirmed by the Fourier transformations of the images which suggest a long period of 15 nm in the AFM-micrograph, and long periods of 12 and 11 nm in the center and right TEM-micrographs, respectively.
Figure 2 is a similar arrangement of micrographs as were shown in Figure 1. The sample, in case of Figure 2, was melt-crystallized at a rate of cooling of 750 K $s^{-1}$. The AFM-image (left) suggests a distinctly non-lamellar geometry of the formed domains. The center and right TEM-images from the center and the surface of the cross-section of the film, respectively, similarly, show absence of well-developed lamellae, independent of the location in the sample. The objects in the TEM-micrographs, occasionally, seem to be non-isotropic and not as distinctly equi-axed as was detected by AFM. Further magnification, as is provided with the insets in the TEM-micrographs reveals alignment of particle-like domains to strings of limited length. The size of domains is about 10-15 nm in the AFM-micrograph, and the short dimension of the domains in the TEM-micrographs is only about 5 nm. The Fourier transformation of the TEM-images yields long periods of 11-12 and 10-12 nm for the bulk and surface regions, respectively.

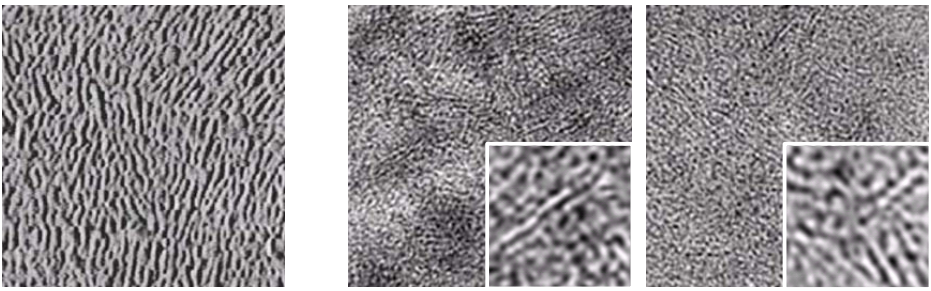

**Figure 1.** AFM-structure (left) and TEM-structure (center and right) of iPP, which was melt-crystallized at 12 K $s^{-1}$. The images show an area of 500 nm × 500 nm. The insets in the TEM-micrographs correspond to an area of 100 nm × 100 nm. The TEM-images were taken in the center of the sample (center image) and near the surface (right image).

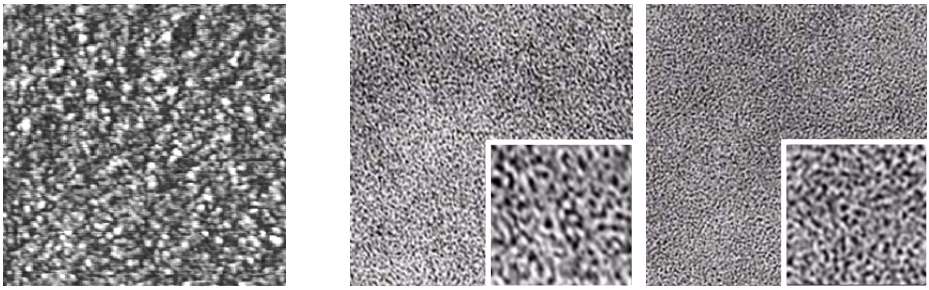

**Figure 2.** AFM-structure (left) and TEM-structure (center and right) of iPP, which was melt-crystallized at 750 K $s^{-1}$. The images show an area of 500 nm × 500 nm. The insets in the TEM-micrographs correspond to an area of 100 nm × 100 nm. The TEM-images were taken in the center of the sample (center image) and near the surface (right image).

Figure 3 is a comparison of the AFM-structure (left) and TEM-structure (right) of an annealed sample of iPP. The initial melt-crystallization was performed at a rate of cooling of 750 K $s^{-1}$, and the annealing was done at a temperature of 393 K, for a period of 60 min. The morphology of the specimen, before annealing, i.e., at ambient temperature, after melt-crystallization, was shown in Figure 2. Melt-crystallization at 750 K $s^{-1}$ yielded non-lamellar, mesomorphic domains, which, on heating to the annealing temperature, transform to monoclinic crystals of nearly identical geometry. The AFM-image of Figure 3 suggests a slight increase of the size of crystals from initially less than 15 nm to about 20-25 nm as a result of isothermal annealing at 393 K, with the shape almost unchanged. The corresponding TEM-image supports the preservation of the shape of crystals, despite the observed size is again considerably smaller than suggested by the AFM-analysis. Though a quantitative analysis of the TEM-crystal size is complicated, since crystals apparently are not isolated, the dimensions seem to be not larger than 10 nm. Figure 3 does not include the comparison of surface and bulk structures, as was provided with the center and right images in Figures 1 and 2. We assume that isothermal annealing does not cause a temperature gradient which would require such a comparison. The images of Figures 1 and 2, furthermore, revealed that the initial structure before annealing is almost independent on the location in the film.

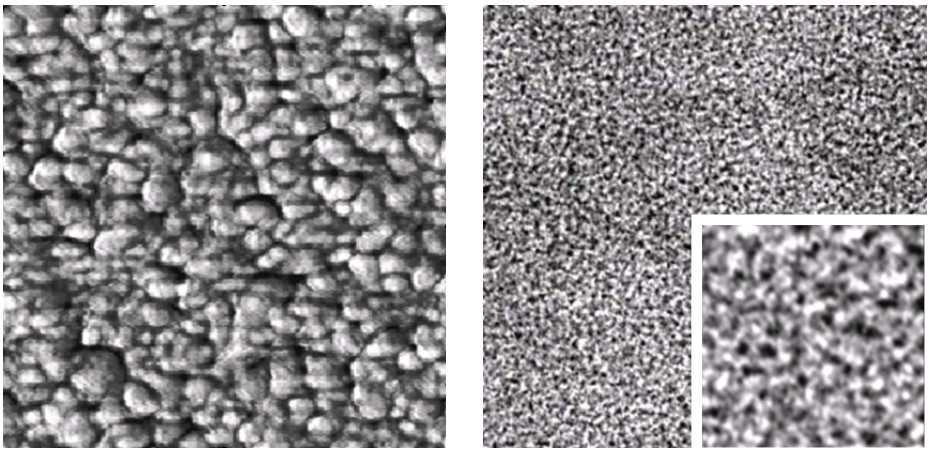

**Figure 3.** AFM-structure (left) and TEM-structure (right) of iPP, which was melt-crystallized at 750 K $s^{-1}$, and annealed for a period of 60 min at 393 K. The images show an area of 500 nm × 500 nm, and the inset in the TEM-micrograph corresponds to an area of 100 nm × 100 nm.

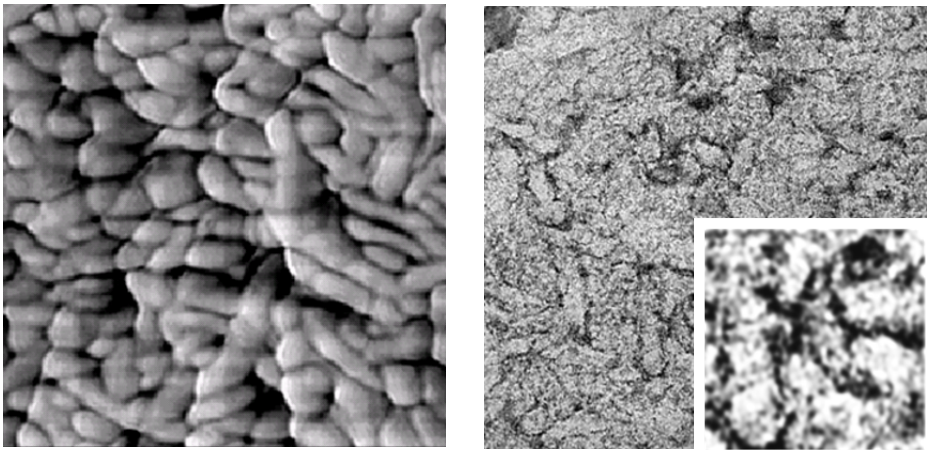

**Figure 4.** AFM-structure (left) and TEM-structure (right) of iPP, which was melt-crystallized at 750 K $s^{-1}$, and annealed for a period of 60 min at 433 K. The images show an area of 500 nm × 500 nm, and the inset in the TEM-micrograph corresponds to an area of 100 nm × 100 nm.

Figure 4 shows the effect of isothermal annealing at 433 K for 60 min of an identical preparation of iPP, i.e., of a sample which initially was melt-crystallized at 750 K $s^{-1}$. The left and right images, as before, show the AFM-structure and the TEM-structure, respectively, after annealing. Most striking is the observation of an increased aspect ratio and size of crystals in both, AFM and TEM analyses. The shorter dimension of crystals is 20-40 nm in the AFM-micrograph and about 20-30 nm in the TEM-image. Whereas the AFM-image does not permit further interpretation, and does not reveal additional insight of the structure, the TEM-image provides additional space for speculative discussions. We are able to detect large domains of similar geometry as obtained by AFM. The surface of these large heterogeneities, however, is structured

and not as smooth as in the AFM-micrograph. Furthermore, the large domains seem to consist of smaller units, and being not homogeneous as is suggested by AFM-analysis.

## Discussion

The present study is a continuation of recent research about the structure and morphology of crystals in iPP, formed on fast melt-crystallization. Rapid cooling of the melt yields mesomorphic domains of non-lamellar shape, which transform on subsequent heating to monoclinic crystals. Simultaneously, heating and/or isothermal annealing at elevated temperature allows reorganization of crystals. The effect of cooling rate on primary crystallization, and the effects of temperature and time of annealing on the phase morphology and crystal morphology were fully evaluated and explained from point-of-view of phenomenology. Uncertainty remained due to preferred analysis of the structure at the nanometer scale by surface-sensitive AFM. To rule out (a) instrumental effects on the analysis of the morphology of crystals, and (b) differences between surface and bulk structures, in this study TEM was employed for verification of former AFM-results.

The experimental results of this investigation, throughout, show coincidence of AFM and TEM results regarding the shape of domains or crystals, respectively. The transition from a lamellar crystal geometry (Figure 1) to a nodular crystal geometry (Figure 2), by an increase of the cooling rate on primary melt-crystallization, is clearly identified by AFM and TEM. Furthermore, TEM confirms the reorganization of crystals by annealing at elevated temperature. The initially mesomorphic nodules after fast cooling at 750 K $s^{-1}$ (Figure 2) increase in size as a function of the annealing temperature (Figures 3 and 4).

Major mismatch between AFM and TEM is observed regarding the absolute size of crystals. In general, TEM yields smaller dimensions of objects than AFM. The percentage difference of the size of objects seems to decrease with an increasing absolute size of crystals. In other words, if the absolute size of crystals is less than 10-20 nm, as in case of the preparation shown in Figure 2, then AFM shows about 100% larger values than TEM. If the absolute size of objects gets larger about 20-30 nm, as is achieved by annealing at 433 K (Figure 4), then AFM yields only slightly larger values than TEM. A rather straightforward explanation of this observation is the limited spatial resolution of the AFM since the radius of the used tip for scanning is about 10 nm. The limited spatial resolution of the used instrumental setup may also be the reason for the rather homogenous and smooth appearance of objects in AFM. TEM, in contrast, apparently, is able to visualize finer details at a length scale below 10 nm. An example is the fine-structure of lamellae in Figure 1, which seem to be composed of aligned spherical objects. An explanation of the observation of heterogeneous lamellae is beyond the scope of the present study, however, is possible with existing models of the polymer-crystallization process [18,19].

Furthermore, differences between AFM and TEM structures may be caused by the presence of a rigid amorphous structure [20]. In general, the amorphous phase in semi-crystalline polymers may partially be immobilized due to the covalent coupling of phases at the phase boundary, i.e., at the crystal basal planes. AFM phase-mode imaging cannot distinguish between the crystalline phase and a glassy, immobilized amorphous phase, since the mechanical response of both structures would be similar. Image-contrast in TEM is based on the penetration of the staining agent. Since the free

volume of the amorphous phase, regardless its mobility, is distinctly larger than the free volume of the crystal phase, for accommodation of the staining agent, presence of an immobilized fraction of the amorphous phase probably does not affect the TEM structure.

The TEM-micrographs in Figures 1 and 2 provide valuable information that the surface and bulk structures across the film of thickness of 100 μm are indifferent. This result proves that the conditions of cooling during primary melt-crystallization at the surface and in the interior of the polymer film are sufficiently small to have a major effect on structure formation. This result is expected from theoretical estimations, and polarizing-optical-microscopy images [21]. Secondly, the coincidence of the structure at the surface and in the interior of the polymer film, points to absence of an effect of the glass-substrate on structure formation/crystallization at the surface.

## Conclusions

TEM and AFM, qualitatively, yield identical information about the morphology of crystals of initially rapidly cooled and subsequent at elevated temperature annealed iPP. Fast melt-crystallization leads to formation of non-lamellar domains of size of 10-20 nm, which grow on subsequent heating as a function of temperature. The observed maximum size of crystals of 40 nm is achieved by annealing at 433 K. The morphology of crystals is uniform across the cross-section of the sample, and the crystallization at the surface is not affected by the use of glass as substrate for preparation of films. AFM-analysis, consistently, suggests larger size of heterogeneities than TEM-analysis. The mismatch increases with decreasing absolute size of objects, which allows to identify the geometry of the tip as major reason. Objects of size lower than about 10 nm cannot be resolved or even quantitatively analyzed, respectively, by AFM, when equipped with standard tips with a radius of curvature of around 10 nm.

## References

1. Natta G (1960) Makromolekulare Chemie 35:94
2. Piccarolo S (1992) J Macromol Sci, Phys B31:501
3. Zia Q, Androsch R, Radusch HJ, Piccarolo S (2006) Polymer 47:8163
4. Zia Q, Radusch HJ, Androsch R (2007) Polymer 48:3504
5. Magonov SN, Reneker DH (1997) Annual Rev Mater Sci 27:175
6. Wunderlich B (1976) Crystal nucleation, growth, annealing, In: Macromolecular Physics, Vol 2, Academic Press, New York
7. Feng J, Chen M, Huang Z, Guo Y, Hu H (2002) J Appl Pol Sci 85:1742
8. Cho K, Kim D, Yoon S (2003) Macromolecules 36:7652
9. Zhou H, Wilkes GL (1997) Polymer 38:5735
10. Kathryn A, Ramirez A, Kathy LR (1998) Langmuir 14:2562
11. Stocker W, Beckmann J, Stadler R, Rabe J (1996) Macromolecules 29:7502
12. Radovanovic EA, Carone E, Gonc MC, Alves B (2004) Polymer Testing 23:231
13. Lagerpusch U, Anczykowski B, Nembach E (2001) Philosophical magazine A 81:2613
14. Zeng X, Koshizaki N, Sasaki T (1999) Appl Phys A 69:253
15. Jandt KD (1998) Mat Sci Eng R21:221
16. Strobl GR (1981) J Pol Sci, Pol Phys 21:1357
17. Montezinos D, Wells BG, Burns JL (1985) J Pol Sci, Letters 23:421

18. Goderis B, Reynaers H, Scherrenberg R, Mathot VBF, Koch MJ (2001) Macromolecules 34:1779
19. Strobl G (2006) Progr Polym Sci 31:398
20. Menczel J, Wunderlich B (1981) J Pol Sci, Pol Letters 19:261
21. Brucato V, Piccarolo S, La Carruba V (2002) Chem Eng Sci 57:4129